Effect of RuAl and TiN Underlayers on Grain Morphology, Ordering, and Magnetic Properties of FePt-SiO_x Thin Films

Hoan Ho[1,2], David E. Laughlin[1,2,3], and Jian-Gang Zhu[1,2,3]

[1]Data Storage Systems Center, Carnegie Mellon University, Pittsburgh, PA 15213 USA
[2]Materials Science and Engineering Department, Carnegie Mellon University, Pittsburgh, PA 15213 USA
[3]Electrial and Computer Engineering Department, Carnegie Mellon University, Pittsburgh, PA 15213 USA

The impact of RuAl underlayers and TiN intermediate layers on the microstructure, $L1_0$ ordering, and coercivity of granular FePt thin films is evaluated with an emphasis on controlling the FePt grains by using a new underlayer system. The use of the single RuAl/TiN film stacks does not help induce the epitaxial grain pick-up for FePt media due to their overly small grain size and smooth surface morphology. Two-step-deposited RuAl layers are developed to make a more open microstructure. By sputtering the top RuAl layers at low power and high Ar pressure, it is shown that there is a one-to-one grain matching between RuAl/TiN and FePt. It is also found that TiN underlayers are more favorable to the $L1_0$ ordering process compared to MgO underlayers.

Index Terms—**Grain morphology, $L1_0$ FePt, ordering, RuAl, TiN.**

I. Introduction

HIGH anisotropy $L1_0$ FePt is well known to be the most probable magnetic material for Heat Assisted Magnetic Recording (HAMR). FePt grain morphology that includes small grains with narrow size distribution and good boundary isolation directly affects the signal to noise ratio of the media. In conventional perpendicular magnetic recording (PMR), NiW/Ru underlayers help obtain the control of grain size and size distribution for the CoCrPt recording layers [1]. In FePt-based media, polycrystalline MgO [2], [3] and recently TiN [4], [5] have been used as underlayers mainly to provide the c-axis texture for FePt grains and assist the ordering process. They do not function as underlayer-grain-templating. Zhang *et al.* [6] has shown that there are more than two FePt grains nucleating from a single MgO grain in FePtAg-C granular thin films. This is due to large MgO grain size of about 20 nm as can be seen in Fig. 1(a). Some research groups [4], [7] have reported the use of B2 RuAl, which is known for its fine grains, to control FePt grain size. However, there have not yet been clear correlations between the RuAl underlayer grains and FePt medium grains. In this paper, we focus on how the RuAl underlayers influence the morphology of the FePt grains in the FePt-SiO_x recording layers. In addition, the impact of the TiN intermediate layers, which serve as barriers to block interdiffusion between RuAl and FePt, on the $L1_0$ ordering and magnetic properties will also be assessed.

II. Experimental Details

Films were fabricated by RF sputtering, using a Leybold Heraeus Z400 sputtering system at a base pressure $<5\times10^{-7}$ Torr. RuAl (45 nm) underlayers were first grown on naturally oxidized 1 in. Si (001) wafers with a sputtering power of 80 W and under 3 mTorr Ar gas pressure. This was followed by TiN intermediate layers of 0–16 nm thickness deposited at 100 W and 10 mTorr. Subsequently, 10 nm FePt-45 vol.%SiO_x media were sputtered by multilayer deposition from $Fe_{55}Pt_{45}$ and SiO_x targets at 20 W for FePt and 30 W for SiO_x; and 10 mTorr Ar pressure [2]. The thickness of FePt in each step was 0.76 nm and that of SiO_x was 0.62 nm. There were a total of 9 repeats. The deposition rates of RuAl, TiN, FePt, and SiO_x were 1.00 Å/s, 0.60 Å/s, 0.71Å/s, and 0.26 Å/s, respectively. The in-situ heating temperature was 300, 300, and 400 °C for RuAl, TiN, and FePt-SiO_x, respectively.

In the experiments on the effect of TiN on $L1_0$ ordering, the film structures were FePt-50vol.%SiO_x(10 nm)/TiN (6 nm)/MgO (15 nm)/Si substrate. MgO underlayers were deposited at 30 W, 10 mTorr, and room temperature with a deposition rate of 0.15Å/s. The in-situ heating temperature for FePt-SiO_x was varied from 390 to 510 °C. To be consistent, RuAl instead of MgO should have been put down as the underlayers. However, we have some adhesion issues with RuAl on Si wafers at high heating temperature >450 °C, which additionally requires Ta seedlayers. Since we are limited to four targets in the sputtering machine, MgO was alternatively used. Another set of samples with the structure FePt-SiO_x/MgO/Si substrate were fabricated for comparison.

The film texture and microstructure were characterized by X-ray diffraction (XRD) with CuKα radiation and transmission electron microscopy (TEM). The magnetic properties were tested at room temperature by a vibrating sample magnetometer (VSM) with a maximum applied field of 90 kOe.

III. Results and Discussion

The XRD results in Fig. 1(e) show that the 45 nm RuAl layer grown directly onto the Si substrate forms a good (001) texture. The RuAl (110) peak is almost invisible. The composition measurement by energy dispersive spectroscopy from scanning electron microscope shows that the RuAl films have 51 at.% Ru and 49 at.% Al, which is very close to the composition of the $Ru_{50}Al_{50}$ target. The TiN intermediate layers of 16 nm and 6 nm thickness grow on the RuAl underlayers with (002) textures [see Fig. 1(e)]. Because the lattice constants of RuAl and TiN are 2.99 Å and 4.2 Å, respectively, the epitaxial relationship between RuAl and TiN layers is RuAl $(001)[110] \parallel \mathrm{TiN}(002)[100]$. The B2 RuAl is known to be

Manuscript received November 05, 2012; accepted December 17, 2012. Date of current version July 15, 2013. Corresponding author: H. Ho (hoanh@andrew.cmu.edu).

Color versions of one or more of the figures in this paper are available online at http://ieeexplore.ieee.org.

Digital Object Identifier 10.1109/TMAG.2012.2236681

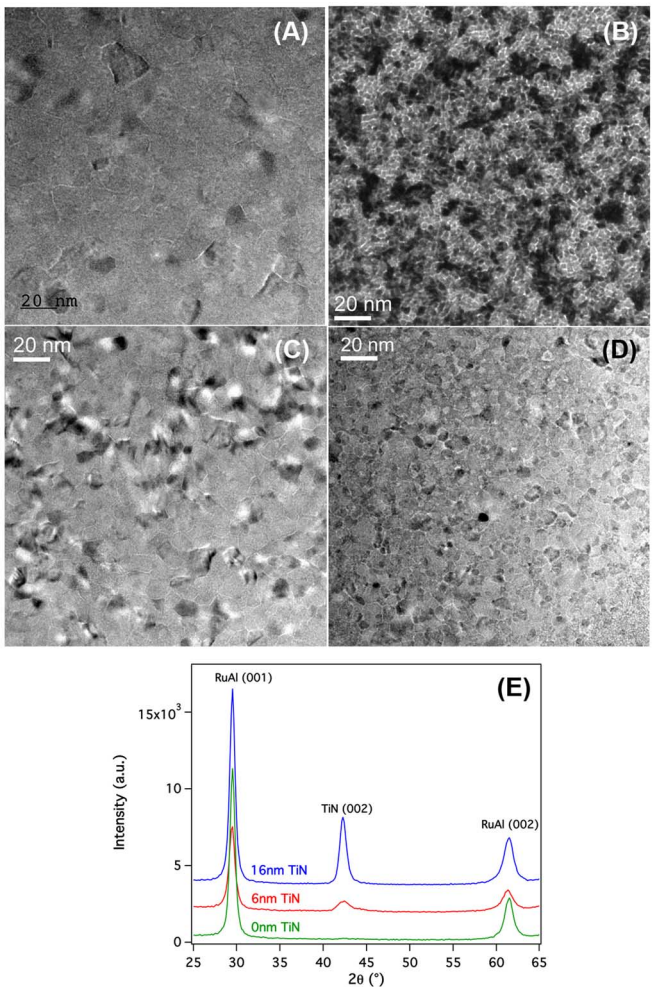

Fig. 1. Plane view TEM images of (a) 15 nm thick MgO deposited at room temperature, (b) 45 nm thick RuAl, (c) 16 nm thick TiN deposited on RuAl, and (d) 6 nm thick TiN deposited on RuAl. (e) XRD patterns of TiN with varying thickness on 45 nm RuAl.

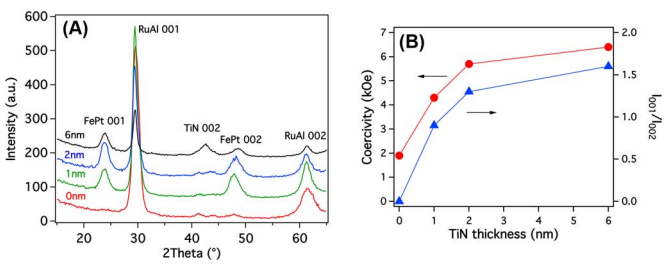

Fig. 2. (a) XRD patterns of FePt-45 vol.%SiO_x (10 nm)/TiN (X nm)/RuAl (45 nm) (X = 0–6 nm). (b) Coercivity H_c and ratio I_{001}/I_{002} as a function of TiN intermediate layer thickness.

highly stable due to a strong bonding between the Ru and Al atoms. For that reason, RuAl exhibits a small grain size of ~5–6 nm for the 45 nm film as viewed in the plane view TEM image [see Fig. 1(b)]. TiN deposited on RuAl also shows fairly small grains, which depend on the TiN layer thickness. The grain size decreases from ~10 nm to ~7 nm as TiN thickness is reduced from 16 nm to 6 nm [see Fig. 1(c) and (d)]. Although it is difficult to quantify the grain size for thinner TiN, we believe

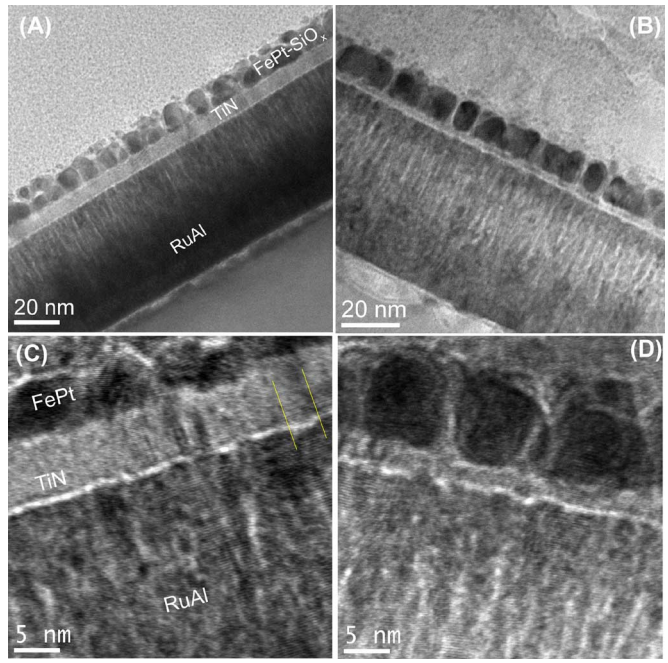

Fig. 3. Cross section TEM images of FePt-SiO_x/TiN (X nm)/RuAl with (a) X = 6 nm and (b) X = 2 nm. Corresponding high-resolution TEM images for (c) X = 6 nm and (d) X = 2 nm.

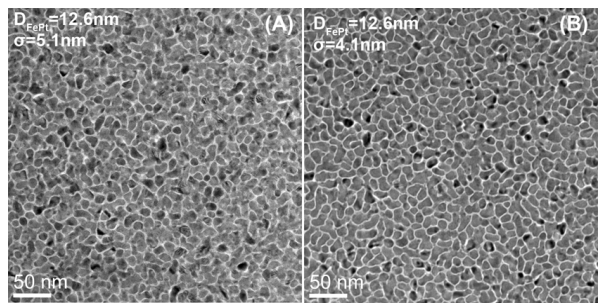

Fig. 4. Plane view TEM images of FePt-SiO_x media in FePt-SiO_x/TiN (X nm)/RuAl with (a) X = 6 nm and (b) X = 2 nm. Insets are the average FePt grain size and size distribution.

smaller thickness enables TiN to copy the grain size of the RuAl underlayers.

The XRD spectra of FePt-SiO_x/TiN (X nm)/RuAl with X = 0–6 nm [Fig. 2(a)] reveal the perpendicular texture of FePt films on 6 to 1 nm thick TiN. The integral intensity ratio of FePt (001) and FePt (002) peaks, I_{001}/I_{002}, decreases with thinner TiN layers [see Fig. 2(b)]. The degradation of $L1_0$ ordering gives rise to a corresponding decrease in coercivity with TiN thickness. Without inserting the TiN layer, the ratio I_{001}/I_{002} becomes zero with no obvious FePt (001) observed in the XRD scan. It has been reported that RuAl and FePt interdiffuse and deteriorate the $L1_0$ chemical ordering and magnetic properties of the FePt media [4], [7]. Since TiN works as a barrier to block that interdiffusion, TiN thickness is critical. TiN layers are necessary to be thin for small crystalline size requirement, but they have to be thick enough to prevent interdiffusion between RuAl and FePt. The 2 nm thickness does not cause a significant reduction in the chemical ordering and H_c of the FePt films compared to the 6 nm thickness, hence, 2 nm thick TiN is optimal.

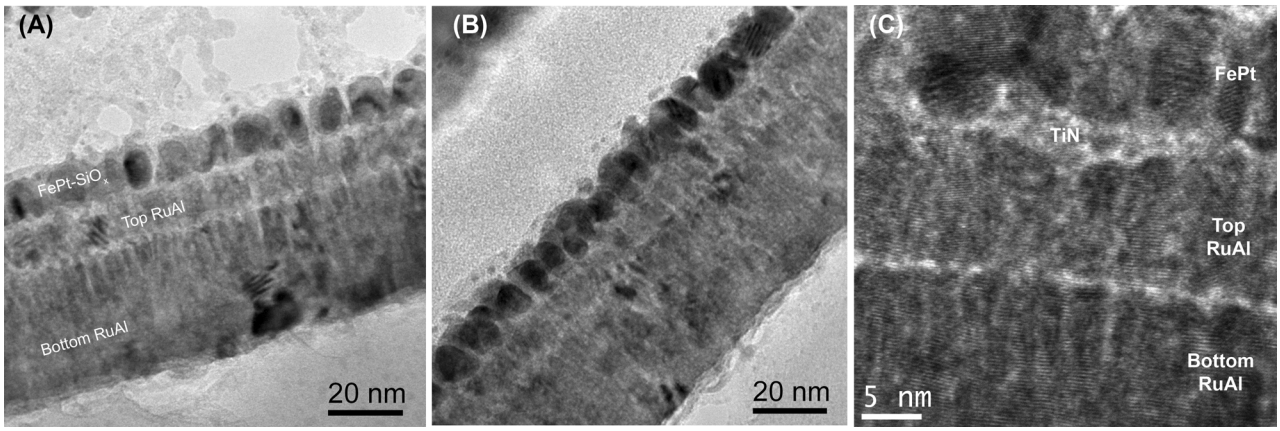

Fig. 5. Cross section TEM images of FePt-45vol.%SiO_x (10 nm)/TiN (2 nm)/Top RuAl (15 nm)/Bottom RuAl (30 nm) with the top RuAl sputtered at (a) 40 W and 30 mTorr, and (b) 20 W and 30 mTorr. (c) High resolution TEM image of the sample in (b).

It can be clearly seen in Fig. 3(a) and (b) that RuAl develops small and columnar grains. This is a promising template for controlling the grain growth of the FePt films. The cross-section high-resolution TEM images in Fig. 3(c) and (d) indicate an excellent epitaxial growth all the way from RuAl to TiN and to FePt media in the case of 6 nm and even 2 nm thick TiN intermediate layers. It is also clear that TiN grains pick up and grow from underneath RuAl grains. Nevertheless, the grains in the FePt overlayer are much larger, and one FePt grain actually overgrows on top of more than one grain from the underlayers. It is attributed to the fact that the grains of RuAl and TiN are too small and the surface of RuAl and TiN are fairly smooth due to the low Ar sputtering pressure. Consequently, it is difficult for FePt to develop a grain-to-grain growth relationship with the RuAl/TiN underlayers. From the plane-view TEM images (see Fig. 4), we see very similar grain size of the FePt-SiO_x media deposited on 6 nm and 2 nm thick TiN layers. The average grain size is all 12.6 nm.

The double RuAl layer structure was employed to create a more open microstructure. RuAl with slightly larger grain size and bumpier surface morphology would facilitate FePt grains to nucleate and follow the underlayer grain template. Bottom RuAl layers of 30 nm were deposited at the same sputtering conditions and served to support the texture for the top RuAl layers. The 15 nm thick RuAl overlayers were sputtered at high Ar working pressure of 30 mTorr and low powers of 40 and 20 W for obtaining larger grains and more dome-shaped surface. 2 nm thick TiN was inserted between FePt and the top RuAl. The high resolution TEM [see Fig. 5(c)] of the double RuAl structure demonstrates a good epitaxial growth between the bottom and top RuAl layers. More importantly, by using the new sputtering conditions, the grains in the top layer now become larger than those in the bottom, and the interface is rougher as viewed from the cross-section images in Fig. 5(a) and (b). The 2 nm thick TiN appears to conform to the surface morphology of RuAl. This more open microstructure helps induce a one-to-one grain relationship between FePt and TiN/RuAl, which is clearly shown in Fig. 5(a) and (b). From the top view [see Fig. 6], however, the FePt grains still coalesce and interconnect to one another. It has been studied that SiO_x does not well segregate to the FePt grain boundaries to encircle the grains [8]. In this case, even if

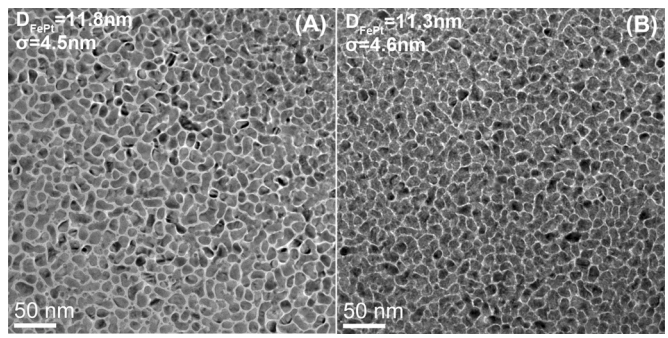

Fig. 6. Plane view TEM images of FePt-SiO_x media in the double RuAl films with top RuAl sputtered at (a) 40 W and 30 mTorr, and (b) 20 W and 30 mTorr. Insets are the average FePt grain size and size distribution.

the RuAl underlayers with physically well-separated columns realize one-to-one grain matching between RuAl and FePt, the FePt-SiO_x granular films still form the maze-like microstructure. Other amorphous segregants need to be sought for a better grain boundary isolation.

Fig. 7(a) plots the order parameter, S, as a function of deposition temperature of the FePt-SiO_x films sputtered on the TiN/MgO and pure MgO underlayers. S was calculated from the ratio I_{001}/I_{002} with the absorption factor and Lorentz factor taken into account [9]. Except for the low deposition temperature regime, 390 °C and 410 °C, the $L1_0$ ordering of FePt on TiN/MgO is better than on MgO. This comes from the fact that the lattice constant of TiN (4.242 Å) is slightly larger than that of MgO (4.211 Å). TiN imposes more tensile stress onto the FePt basal plane to compress the c-axis more, and hence further drive the $L1_0$ ordering process. The better $L1_0$ ordering leads to higher coercivity H_c of FePt on TiN than on MgO as shown in Fig. 7(b). The discrepancies at 390 °C and 410 °C are likely because weak FePt (001) peaks at low chemical ordering make peak fitting and hence calculation of S less precise. Interestingly, at the high temperature regime (470 °C–510 °C), while the H_c values increase dramatically with temperature for the MgO case, they tend to flatten out for the TiN/MgO case. We speculate that TiN may diffuse into FePt at elevated temperature and degrade the magnetic properties of FePt, which becomes

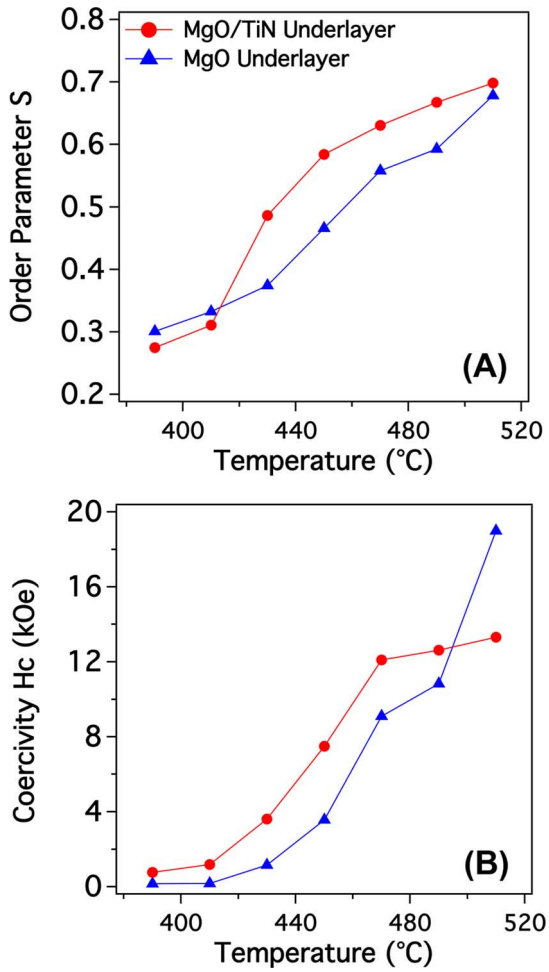

Fig. 7. (a) Order parameter S and (b) coercivity H_c versus deposition temperature for FePt-SiO_x films on TiN/MgO and MgO.

more severe with higher temperature. This observed phenomenon will be further investigated in detail.

IV. Conclusion

RuAl films with good (001) texture and small and separating columnar grains have been successfully fabricated directly on Si substrates. Microstructure of the films in terms of grain size and surface morphology can be tuned by changing sputtering conditions. It has also been demonstrated that the small grains transfer from the RuAl underlayers to the TiN intermediate barriers. Although the double RuAl film stacks can promote the grain matching with the FePt-SiO_x media, the FePt grain isolation does not show obvious improvement. TiN is better at assisting the $L1_0$ ordering process than MgO. However, there may be an interdiffusion concern between TiN and FePt when the films are sputtered at high temperature above 470°C.

Acknowledgment

This work was supported in part by Seagate Technology, Western Digital, and the Data Storage Systems Center of Carnegie Mellon University. The authors would like to thank them for their funding and fruitful discussions.

References

[1] R. Mukai, T. Uzumaki, and A. Tanaka, "Signal-to-media-noise ratio improvement of CoCrPt-SiO_2 granular perpendicular media by stacked Ru underlayer," *J. Appl. Phys.*, vol. 97, p. 10N119, 2005.

[2] Y. Peng, J.-G. Zhu, and D. E. Laughlin, "$L1_0$ FePt-MgO perpendicular thin film deposited by alternating sputtering at elevated temperature," *J. Appl. Phys.*, vol. 99, p. 08F907, 2006.

[3] A. Perumal, Y. K. Takahashi, and K. Hono, "$L1_0$ FePt-C nanogranular perpendicular anisotropy films with narrow size distribution," *Appl. Phys. Exp.*, vol. 1, p. 101301, 2008.

[4] E. Yang, S. Ratanaphan, D. E. Laughlin, and J. G. Zhu, "Highly ordered FePt $L1_0$ thin films with small grains on RuAl seed layers," *IEEE Trans. Magn.*, vol. 47, no. 1, pp. 81–86, Jan. 2011.

[5] H. H. Li, K. F. Dong, Y. G. Peng, G. Ju, G. M. Chow, and J. S. Chen, "High coercive FePt and FePt-SiN_x(001) films with small grain size and narrow opening-up of in-plane hysteresis loop by TiN intermediate layer," *J. Appl. Phys.*, vol. 110, p. 043911, 2011.

[6] L. Zhang, Y. K. Takahashi, K. Hono, B. C. Stipe, J. Juang, and M. Grobis, "FePtAg-C nanogranular film as thermally assisted magnetic recording (TAR) media," *IEEE Trans. Magn.*, vol. 47, no. 10, pp. 4062–4065, Oct. 2011.

[7] W. K. Shen, J. H. Judy, and J.-P. Wang, "In situ epitaxial growth of ordered FePt (001) films with ultra small and uniform grain size using a RuAl underlayer," *J. Appl. Phys.*, vol. 97, pp. 10H301–10H303, 2005.

[8] E. Yang, H. Ho, D. E. Laughlin, and J.-G. Zhu, "Columnar grain growth of FePt($L1_0$) thin films," *J. Appl. Phys.*, vol. 111, p. 07B720, 2012.

[9] E. Yang, D. E. Laughlin, and J. G. Zhu, "Correction of order parameter calculations for FePt perpendicular thin films," *IEEE Trans. Magn.*, vol. 48, no. 1, pp. 7–12, Jan. 2012.